

This article was downloaded by:

On: 14 January 2011

Access details: *Access Details: Free Access*

Publisher *Taylor & Francis*

Informa Ltd Registered in England and Wales Registered Number: 1072954 Registered office: Mortimer House, 37-41 Mortimer Street, London W1T 3JH, UK



## Molecular Simulation

Publication details, including instructions for authors and subscription information:

<http://www.informaworld.com/smpp/title~content=t713644482>

### Effect of cut-off distance used in molecular dynamics simulations on fluid properties

Cunkui Huang<sup>a</sup>; Chunli Li<sup>b</sup>; Phillip Y. K. Choi<sup>b</sup>; K. Nandakumar<sup>c</sup>; Larry W. Kostiuk<sup>d</sup>

<sup>a</sup> Alberta Innovates - Technology Futures, Edmonton, Alberta, Canada <sup>b</sup> Department of Chemical and Materials Engineering, University of Alberta, Edmonton, Alberta, Canada <sup>c</sup> Cain Department of Chemical Engineering, Louisiana State University, Baton Rouge, LA, USA <sup>d</sup> Department of Mechanical Engineering, University of Alberta, Edmonton, Alberta, Canada

Online publication date: 15 October 2010

**To cite this Article** Huang, Cunkui , Li, Chunli , Choi, Phillip Y. K. , Nandakumar, K. and Kostiuk, Larry W.(2010) 'Effect of cut-off distance used in molecular dynamics simulations on fluid properties', *Molecular Simulation*, 36: 11, 856 — 864

**To link to this Article:** DOI: 10.1080/08927022.2010.489556

**URL:** <http://dx.doi.org/10.1080/08927022.2010.489556>

PLEASE SCROLL DOWN FOR ARTICLE

Full terms and conditions of use: <http://www.informaworld.com/terms-and-conditions-of-access.pdf>

This article may be used for research, teaching and private study purposes. Any substantial or systematic reproduction, re-distribution, re-selling, loan or sub-licensing, systematic supply or distribution in any form to anyone is expressly forbidden.

The publisher does not give any warranty express or implied or make any representation that the contents will be complete or accurate or up to date. The accuracy of any instructions, formulae and drug doses should be independently verified with primary sources. The publisher shall not be liable for any loss, actions, claims, proceedings, demand or costs or damages whatsoever or howsoever caused arising directly or indirectly in connection with or arising out of the use of this material.

## Effect of cut-off distance used in molecular dynamics simulations on fluid properties

Cunkui Huang<sup>a</sup>, Chunli Li<sup>b</sup>, Phillip Y.K. Choi<sup>b\*</sup>, K. Nandakumar<sup>c</sup> and Larry W. Kostiuk<sup>d</sup>

<sup>a</sup>Alberta Innovates – Technology Futures, Edmonton, Alberta, Canada T6N 1E4; <sup>b</sup>Department of Chemical and Materials Engineering, University of Alberta, Edmonton, Alberta, Canada T6G 2G6; <sup>c</sup>Cain Department of Chemical Engineering, Louisiana State University, Baton Rouge, LA 70803, USA; <sup>d</sup>Department of Mechanical Engineering, University of Alberta, Edmonton, Alberta, Canada T6G 2G8

(Received 9 October 2009; final version received 20 April 2010)

The effect of cut-off distance used in molecular dynamics (MD) simulations on fluid properties was studied systematically in both canonical (NVT) and isothermal–isobaric (NPT) ensembles. Results show that the cut-off distance in the NVT ensemble plays little role in determining the equilibrium structure of fluid if the ensemble has a high density. However, pressures calculated in the same NVT ensembles strongly depend on the cut-off distance used. In the NPT ensemble, cut-off distance plays a key role in determining fluid equilibrium structure, density and self-diffusion coefficient. The characteristic of the radial distribution function of fluid in NPT ensembles depending on the cut-off distance used in MD simulations means that the WCA theory (a perturbation theory developed by Weeks, Chandler and Andersen) is not suitable for NPT ensembles because the assumption (the effect of the attractive force in determining the liquid structure is negligible) used in the WCA theory is not valid. The dependence of fluid properties on the cut-off distance also indicates that using the WCA potential (the repulsive part of the intermolecular potential proposed in the WCA theory) to calculate fluid transport in heterogeneous systems could lead to significant errors or incorrect results.

**Keywords:** molecular dynamics; role attractive force; canonical ensemble; isothermal–isobaric ensemble

### 1. Introduction

The Weeks, Chandler and Andersen (WCA) theory, a perturbation theory developed by Chandler et al. [1], Chandler and Weeks [2] and Weeks and Chandler [3], has been applied to study liquid structures and thermodynamic properties by many researchers [4–7]. In this theory, there are two key assumptions: the first is that the intermolecular potential can be split into a short-range repulsive portion and a longer-range attractive portion; the second is that the effect of the attractive portion in determining the liquid structure is negligible. As a result, the liquid structure and its thermodynamic properties are determined by a radial distribution function (RDF),  $g_0(r)$ , of a repulsive reference liquid that is related to the hard sphere liquid. Weeks et al. compared the  $g_0(r)$  obtained from a repulsive reference fluid and  $g(r)$  of a Lennard-Jones fluid obtained by the molecular dynamics (MD) simulation [8]. The agreement between  $g_0(r)$  and  $g(r)$  is excellent for systems at high densities. In the literature, the repulsive part of the intermolecular potential proposed in the WCA theory has been referred to as the WCA potential and used frequently in the MD simulation [9–13].

The major difference between the WCA potential and the Lennard-Jones potential is that the former does not include the attractive part, while the latter accounts for its effects. Travis and Gubbins [9] studied the Poiseuille flow of Lennard-Jones fluids in narrow slit pores.

They calculated streaming velocities in the pore by using the WCA potential and the Lennard-Jones potential (truncated at  $2.5\sigma$ ) separately. Their results show that the streaming velocity distributions obtained by the two different potentials are not consistent, which means that ignoring the attractive force in the WCA potential impacts the fluid transport through narrow pores. To gain further insights into the effect of the attractive forces (expressed by the cut-off distance in this study) on liquid properties, two ensembles, canonical (NVT) and isothermal–isobaric (NPT) ensembles, were studied. The results for a high-density NVT ensemble show that the cut-off distance used in MD simulations has an insignificant influence on  $g(r)$ , which is consistent with the assumption used in the WCA theory. However, the corresponding pressure calculated from the NVT ensemble was found to be strongly dependent on the cut-off distance used. The results obtained from the NPT ensemble indicate that all properties of a fluid, including the  $g(r)$  and thermodynamic properties, depend significantly on the attractive forces. It means that using the WCA theory in NPT ensembles is difficult because the assumption (i.e. the effect of the attractive force in determining the liquid structure is negligible) used in the WCA theory is not valid. The characteristic of fluid properties depending on the cut-off distance used in MD simulations indicates that using the WCA potential to calculate fluid transport

\*Corresponding author. Email: phillip.choi@ualberta.ca

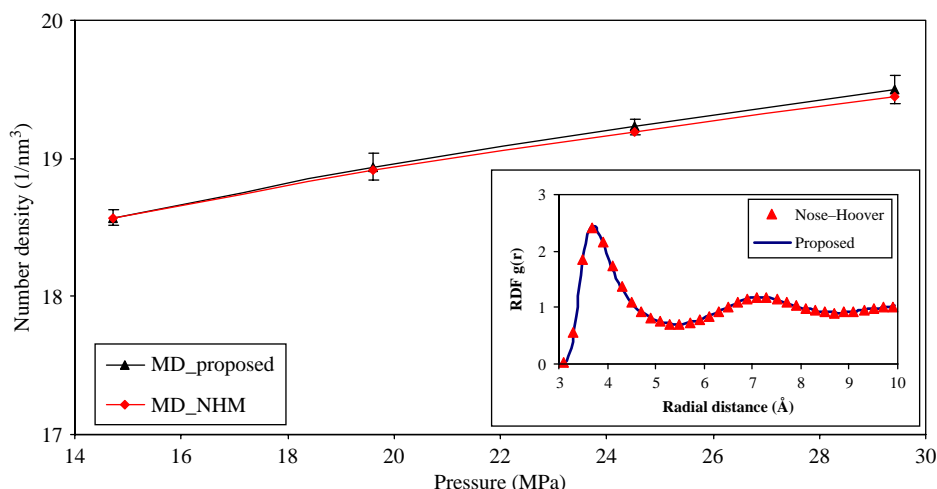


Figure 1. Comparison of number densities in NPT ensembles obtained using the algorithm applied in this paper and the Nose–Hoover method (NHM) under the same temperature (120 K) but different pressures. The symbols  $\blacktriangle$  and  $\blacklozenge$  are the results calculated using the method in this paper and the Nose–Hoover method, respectively. The error bars are the standard deviations corresponding to individual data obtained by the method used in this paper. The inset of the figure is the RDF obtained by two methods at temperature 120 K and pressure 19.6 MPa.

in heterogeneous systems could lead to significant errors or incorrect results.

## 2. Methodology

The equation of state of a fluid on a macroscopic scale signifies the relationship between the temperature, pressure and density. If two of them are fixed, the other will be determined uniquely. To examine the effect of cut-off distance used in MD simulations on the equation of state properties, a Lennard-Jones fluid (i.e. liquid argon) in a state of temperature  $T = 133$  K and pressure  $P = 20$  MPa was chosen. Experimental measurement [14] shows that the density of liquid argon in this state is  $1.19 \text{ g/cm}^3$ , which corresponds to the number density  $\rho_n = 17.93/\text{nm}^3$  or the reduced density  $\rho_n \sigma^3 = 0.708$ , where  $\sigma$  is the length scale of the liquid molecules. Two ensembles (NVT and NPT) were carried out in this study.

For the NVT ensemble, 7733 argon molecules were placed in a cube subjected to periodical boundary conditions in all directions. The average number density of molecules in the cube was set to be the experimental value. The procedure for creating an NVT ensemble was that the molecules were packed in a cube randomly. The initial velocities with a Maxwellian distribution were assigned to them, which corresponded to the system having an average temperature  $T = 133$  K. Then, the thermostat was coupled and the molecules in the system were allowed to move until the equilibration was achieved. After that, the average properties of the fluid were obtained by collecting data over a period of 0.5 ns.

For the NPT ensemble, MD simulations were calculated based on a technique that was proposed by Huang et al. [15–18]. The major feature of this method is that the pressure in the NPT ensemble is maintained by two auto-adjusting boundaries on which two external forces/pressures with the same value are exerted. This method has been validated by comparing the density values and RDF computed at various applied pressures with those obtained from using a well-established Nose–Hoover barostat [19]. Figure 1 illustrates such a comparison. In this figure, the line with symbols  $\blacktriangle$  and error bars are the mean values of density and the standard deviations corresponding to individual points predicted using the current algorithm, while the line with symbols  $\blacklozenge$  signifies the results obtained using the Nose–Hoover barostat. The inset of the figure is an example showing the RDF obtained by the current method (shown by the solid line) and the Nose–Hoover method (shown by symbols  $\blacktriangle$ ) under the same temperature (120 K) and pressure (19.6 MPa). Comparing the densities and RDF obtained by the two methods, one can see that they are consistent.

The procedure for creating an NPT ensemble in the present study consists in an external pressure ( $P_{\text{ext}} = 20$  MPa) being exerted on two auto-adjusting boundaries. These boundaries adjusted their positions automatically according to the forces acting on them. Prior to the data collection, an initial field for each NPT MD simulation run was prepared in such a way so that the mass centre of the system only vibrated around its initial position (i.e. no shifting). For all MD simulations in the NPT ensemble, 10,406 argon molecules were used and periodical boundary conditions were applied in the cross-directions. The dimensions of the

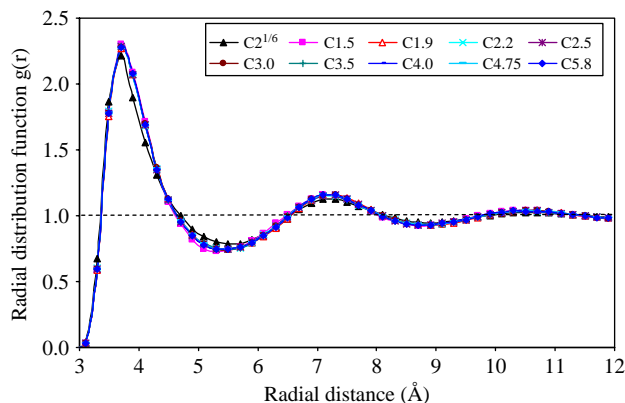


Figure 2. Comparison of RDF obtained using different cut-off distances in an NVT ensemble at temperature  $T = 133$  K and reduced density  $\rho_n \sigma^3 = 0.708$ .

system were  $4 \times 4 \times L \text{ nm}^3$ , where  $L$  is the averaged distance (from 36 to 104 nm) between two auto-adjusting boundaries. To avoid the effects of the two auto-adjusting boundaries on the results, the average properties in this ensemble were collected from the central portion of the system ( $4 \times 4 \times 4 \text{ nm}^3$  cube located at the middle of the two auto-adjusting boundaries) over a period of 1 ns.

Temperature control was achieved by coupling thermostat(s) in the system. Two different thermostats, Berendsen [20] and Nose–Hoover [21], were coupled in a test system to examine their effects on the results, respectively. Comparable thermodynamic properties of the liquid were obtained from these two different thermostats. Therefore, the less computationally demanding Berendsen thermostat was chosen to control the temperature in this work.

### 3. MD simulation

The interaction between two molecules separated by a distance  $r_{ij}$  is modelled by a truncated and shifted Lennard-Jones 12-6 potential:

$$\phi(r_{ij}) = 4\epsilon \left[ \left( \frac{\sigma}{r_{ij}} \right)^{12} - \left( \frac{\sigma}{r_{ij}} \right)^6 \right] - \phi(r_c) \text{ (if } r_{ij} \leq r_c), \quad (1)$$

where  $\sigma$  and  $\epsilon$  are the characteristic length and energy scales, respectively, and  $\phi(r_c)$  is the value of the potential energy at the point of truncation  $r_{ij} = r_c$ . If  $r_{ij} > r_c$ , the potential  $\phi(r_{ij})$  is set to be zero. In this study, we used different cut-off distances to capture the effect of the attractive force on the equilibrated structure and thermodynamic properties of the liquid. If the potential is truncated at  $r_c = 2^{1/6}\sigma$ , only the repulsive force is considered. In this case, Equation (1) represents the WCA potential. If  $r_c > 2^{1/6}\sigma$ , the increasing proportions of the attractive forces are taken into account. In the published

literature, the cut-off distance that is most often used in MD simulations is  $r_c = 2.5\sigma$  [8,9,22–24]. While other cut-off distances, for example,  $r_c = 2.2\sigma$  [25,26],  $3\sigma$  [27] and  $5\sigma$  [28], were used by different authors. In this paper, 10 different cut-off distances ( $r_c = 2^{1/6}$  to  $5.8\sigma$ ) were used to study the impact of the attractive forces on the liquid structure and thermodynamic properties in two different ensembles systematically. The length and energy scales of argon used in the simulations were  $\sigma = 0.34 \text{ nm}$  and  $\epsilon = 1.67 \times 10^{-21} \text{ J}$  [29], respectively.

The equations of motion were integrated using a velocity Verlet algorithm. The stress tensor was calculated by the Irving–Kirkwood equation [30], and the constitutive pressure was defined as minus one-third of the trace of the stress tensor. The self-diffusion constant was calculated using both the Green–Kubo relationship and the Einstein equation [31].

## 4. Results and discussion

### 4.1 Canonical (NVT) ensemble

For NVT ensembles at high densities, the WCA theory has shown that the attractive force has little impact on the equilibrium structure of Lennard-Jones liquids. In this paper, 10 MD simulations using the same NVT conditions, while different cut-off distances ( $r_c = 2^{1/6}$ , 1.5, 1.9, 2.2, 2.5, 3, 3.5, 4, 4.75 and  $5.8\sigma$ ), were performed to examine the effect of cut-off distance (or the attractive forces) on the liquid structure and thermodynamic properties. Figure 2 shows the RDF  $g(r)$  of liquid argon obtained under different truncation distances. In this figure, the curve with symbol  $\blacktriangle$  is  $g_0(r)$  obtained by the pure repulsive force, while others are the results calculated by the combination of the repulsive and partial attractive forces. Comparing the curves plotted in this figure, one can see that  $g(r)$  are essentially the same regardless of the inclusion of the attractive forces in the MD simulations. Here,  $g_0(r)$  produced by the pure repulsive force exhibits identical pattern to other  $g(r)$ , although a slight difference exists. Weeks et al. [3] studied the effect of density on  $g(r)$ . They found that the agreement between  $g_0(r)$  and  $g(r)$  (obtained by MD simulation at  $r_c = 2.5\sigma$ ) was excellent at a high density ( $\rho_n \sigma^3 = 0.85$ ), while the poor agreement between  $g_0(r)$  and  $g(r)$  was observed at a moderate density ( $\rho_n \sigma^3 = 0.5$ ). These two results imply that the agreement between  $g_0(r)$  and  $g(r)$  decreases as the density decreases. In this work, the reduced density is  $\rho_n \sigma^3 = 0.708$ , a slight difference between  $g_0(r)$  and  $g(r)$  is consistent with the results shown by Weeks et al. [3].

Weeks et al. [3] demonstrated that using  $\hat{h}(\kappa)$  (the dimensionless Fourier transform of the correlation function) is better than  $g(r)$  in terms of unravelling the effects of the repulsive and attractive parts of the Lennard-Jones potential on the structure of the liquid. However,

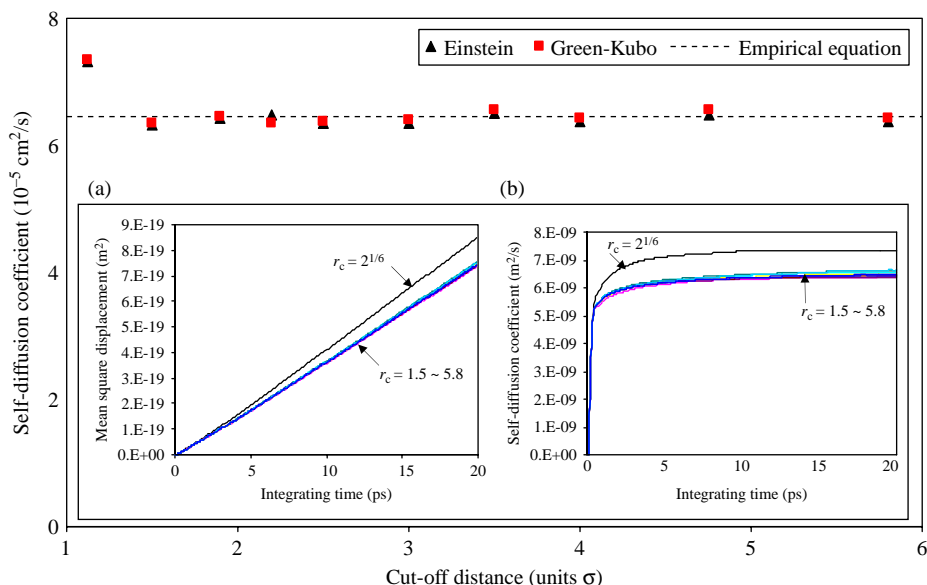


Figure 3. Comparison of self-diffusion coefficients calculated by the Einstein equation, the Green–Kubo relationship and the empirical equation proposed by Naghizadeh and Rice [32] in an NVT ensemble at temperature  $T = 133$  K and reduced density  $\rho_n \sigma^3 = 0.708$ . The insets (a) and (b) of the figure elucidate the mean square displacements and the variations of self-diffusion coefficients calculated using the Green–Kubo relationship under different cut-off distances, respectively.

in the present paper, the intension is not to unravel the effects of different parts of the Lennard-Jones potential. Rather, we compare liquid structures by including different amounts of the attractive forces by varying the cut-off distance.

Naghizadeh and Rice [32] studied the self-diffusion coefficient of liquid argon experimentally. From the

experimental data, they extracted the following empirical equation:

$$\log \tilde{D} = 0.05 + 0.07\tilde{p} - (1/\tilde{T})(1.04 + 0.1\tilde{p}), \quad (2)$$

where  $\tilde{D}$ ,  $\tilde{p}$  and  $\tilde{T}$  are the reduced self-diffusion coefficient, pressure and temperature, which are expressed

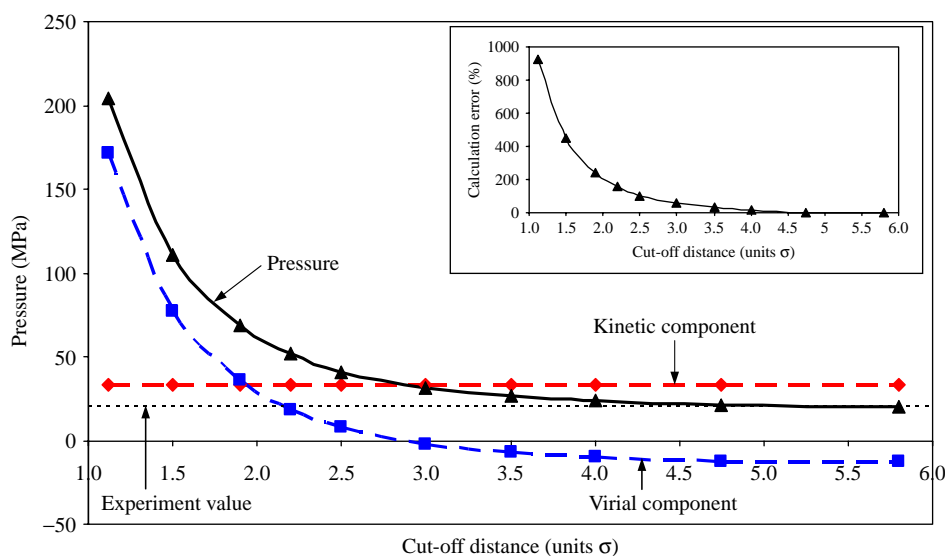


Figure 4. Pressure comparison between the experimental values [14] and MD simulation results obtained at different cut-off distances in an NVT ensemble at  $T = 133$  K and  $\rho_n \sigma^3 = 0.708$ . The dashed lines with symbols  $\blacklozenge$  and  $\blacksquare$  in the figure correspond to the two components (kinetic and virial parts) of pressure, respectively. The inset of the figure shows the simulation error of pressure vs. the cut-off distance.



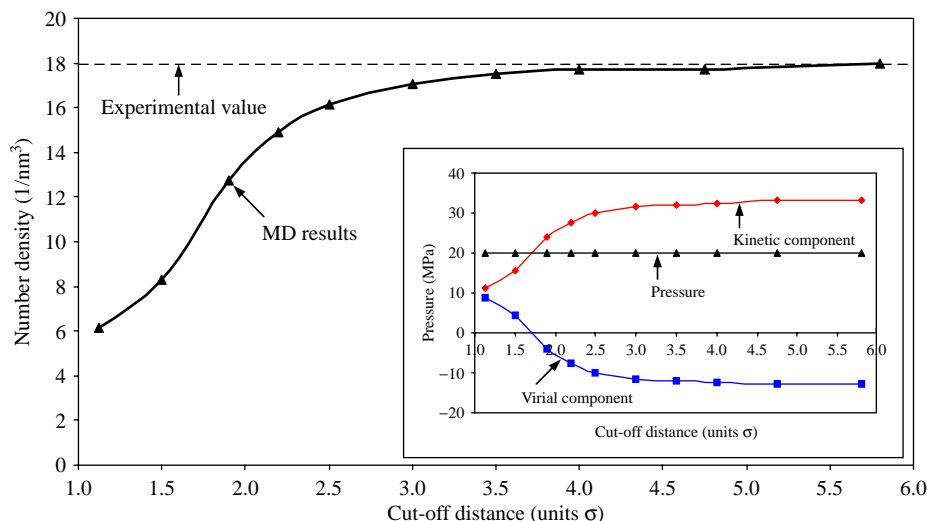


Figure 5. Density comparison between the experimental values [14] and MD simulation results obtained at different cut-off distances in an NPT ensemble at  $T = 133$  K and  $P = 20$  MPa. The inset of the figure is the corresponding distributions of pressure and its two components.

by  $\tilde{D} = [m/(\epsilon\sigma^2)]^{1/2}D$ ,  $\tilde{p} = p\sigma^3/\epsilon$  and  $\tilde{T} = k_bT/\epsilon$ , respectively.

To compare MD simulation results with that obtained by the empirical equation (2), the Einstein equation and the Green–Kubo relationship were applied to calculate the self-diffusion coefficient of liquid argon at the fixed state, respectively. Figure 3 shows the MD simulation results. The insets (a) and (b) in this figure exhibit the variations of the mean square displacements and the self-diffusion coefficients calculated by Green–Kubo relationship vs. the integrating time by using different cut-off distances. In these two insets, one can see that the MD results are almost the same, except for that obtained by applying the pure repulsive force or WCA potential. The self-diffusion coefficients, corresponding to the data shown in the two insets, are exhibited in Figure 3 by symbols  $\blacktriangle$  (Einstein equation) and  $\blacksquare$  (Green–Kubo relationship). The results shown by the symbol  $\blacktriangle$  were obtained using the slope of the mean square displacement between integrating time, 8 and 18 ps; the results shown by the symbol  $\blacksquare$  were the average values over integrating time, 8–18 ps. The dashed line in the figure expresses the values obtained by the empirical equation which was extracted from the experimental data by Naghizadeh and Rice [32]. One can see that the self-diffusion constants calculated by the Einstein equation and Green–Kubo relationship agree well in the whole range of the cut-off distance used. Comparing the self-diffusion coefficients calculated by MD simulations with that obtained by the empirical equation, the agreement between them is fairly good except for the value calculated by considering only the repulsive force. The self-diffusion constant obtained by only accounting for the repulsive force is slightly higher

than the value calculated by using the empirical equation. The difference between them is about 13.6%.

Figures 2 and 3 show that ignoring the attractive forces in the NVT ensemble at a density  $\rho_n\sigma^3 = 0.708$  has essentially no significant impact on the equilibrium structure and self-diffusion coefficient of liquid argon at the chosen state. However, ignoring the attractive forces may impact other properties. To demonstrate this point, pressures in the NVT ensemble at the above-described conditions were calculated by accounting for the effect of the attractive forces. Figure 4 shows the variations of pressure and its two components, kinetic and virial parts, with respect to the cut-off distance. In this figure, the long dashed lines with the symbols  $\blacklozenge$  and  $\blacksquare$ , the solid line with symbols  $\blacktriangle$  and the short dashed line without symbols represent the kinetic component, virial component, total pressure and experimental value [14], respectively. The kinetic component is near constant due to the fact that temperature and density in the NVT ensemble are fixed. But the virial component varies significantly with the cut-off distance used and it dominates the variation of the total pressure. One can see that pressure calculated by only considering the pure repulsive force ( $r_c = 2^{1/6}\sigma$ ) substantially deviates from the real pressure. While as the cut-off distance increases, the difference between the simulation result and the experimental value diminishes. The inset of Figure 4 shows the MD simulation error,  $|P_{MD} - P_{real}|/P_{real}$ , using different cut-off distances. Ignoring the effect of the attractive forces on pressure results in a simulation error of slightly over 900%. It is worth noting that Weeks et al. found that the computed pressure using their theory, not the WCA potential, is comparable to that obtained from the corresponding MD

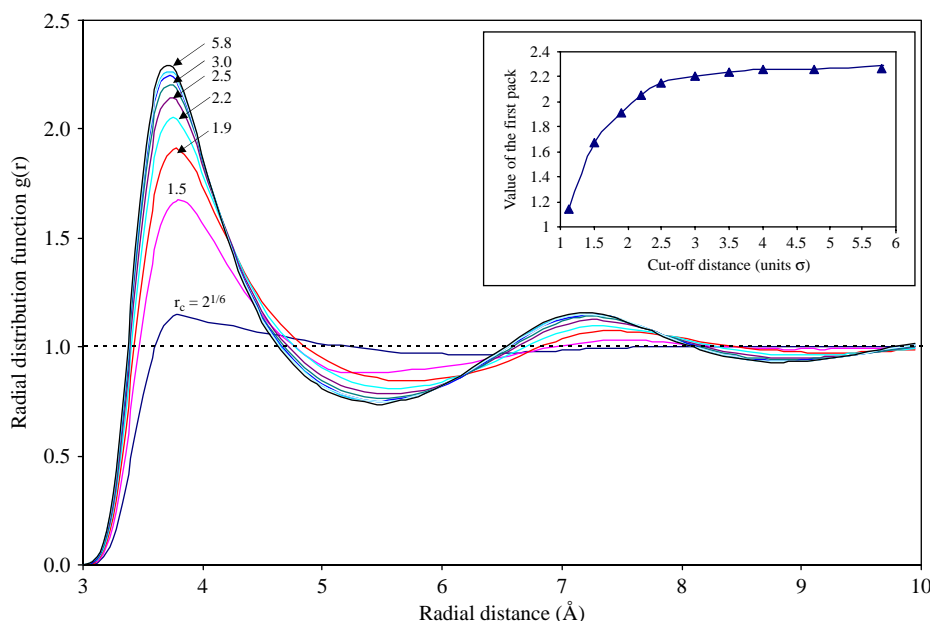


Figure 6. Comparison of RDF obtained using different cut-off distances in an NPT ensemble at  $T = 133$  K and  $P = 20$  MPa. The inset of the figure exhibits the relationship between the first peak value of RDF and cut-off distance.

simulation of a Lennard-Jones fluid [3] as they calculated the pressure by integrating the  $g_0(r)$  from zero to infinity. In this way, the contribution of the attractive forces is implicitly introduced into the calculation. Another noteworthy point is the simulation error using  $r_c = 2.5\sigma$ , a common cut-off distance adopted in MD simulations by many researchers. The error calculated at this truncation is about 104%, which means that the cut-off distance commonly used in MD simulations can predict the liquid equilibrium structure and self-diffusion coefficient properly if the system has a high density condition, while it cannot predict the liquid pressure correctly. To obtain more accurate pressure in MD simulations, a larger cut-off distance should be used. According to Figure 4, to obtain a simulation error for pressure less than 5%, a cut-off distance  $r_c \geq 4.5\sigma$  should be used.

#### 4.2 Isothermal–isobaric (NPT) ensemble

The MD simulation results in the previous section show that the cut-off distance used in an NVT ensemble with high density has no significant influence on the liquid structure and self-diffusion coefficient, but substantially impacts the calculated pressure. Actually, a fluid structure and self-diffusion constant mainly depend on the fluid density, temperature and local free volume, while these parameters in an NVT ensemble at high densities are nearly constant. In this section, a different ensemble (NPT) at the same liquid state, i.e.  $T = 133$  K and  $P = 20$  MPa, is applied to study the role of the cut-off distance used in MD simulations.

Figure 5 and its inset show the variations of density and pressure with respect to the cut-off distance used in the NPT ensemble at the aforementioned conditions. The inset of Figure 5 shows the total pressure and its two components at different truncation distances. One can see that the two components of pressure vary with opposite trends. However, the sum of them (total pressure) stays constant (20 MPa). The effect of the cut-off distance on the density is shown by the solid line with symbols  $\blacktriangle$  in Figure 5. The dashed line in this figure is the experimental value [14]. From this figure, it is noted that the cut-off distance significantly influences the density of the system. When only accounting for the repulsive force ( $r_c = 2^{1/6}\sigma$ ), the density calculated by the MD simulation is much lower than the real value at this state, which means that MD simulations in an NPT ensemble cannot yield a real liquid state if the attractive forces are ignored. As the cut-off distance increases, density increases quickly before a specific cut-off value, e.g.  $r_c < 3\sigma$ . After that, density increases slightly and approaches to a constant value. Comparing with the experimental value, density calculated by the MD simulation at  $r_c = 2.5\sigma$  is lower than the real value by about 10%. If one wants to get more accurate density results, a larger cut-off distance should be applied, e.g.  $r_c \geq 4\sigma$ , resulting in errors  $\leq 2\%$ . Here, the errors of the computed density values vary from 1.2 to 2.4% (95% confidence intervals).

Figure 6 displays the equilibrium structure of liquid argon simulated using the NPT ensemble along with different cut-off distances. In contrast to the RDF obtained in the NVT ensemble, the RDF in the NPT ensemble

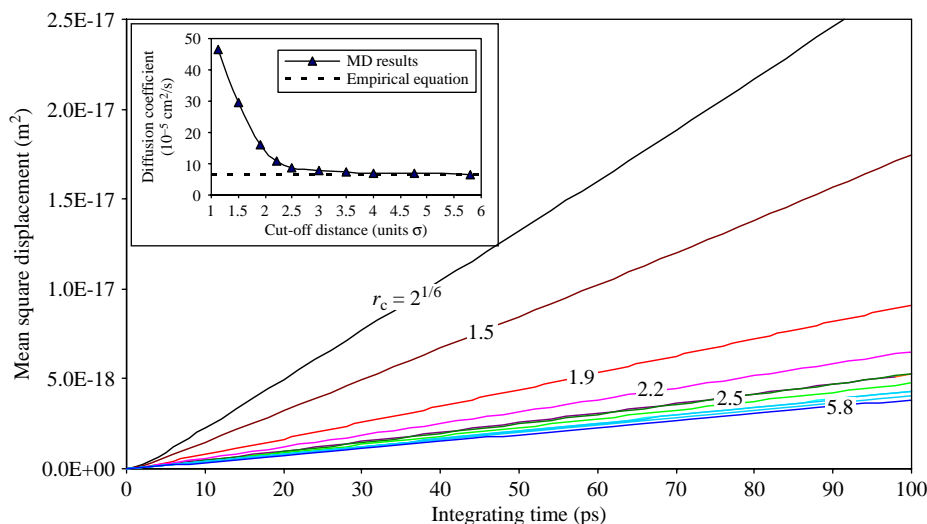


Figure 7. Comparison of mean square displacements obtained at different cut-off distances in an NPT ensemble at  $T = 133 \text{ K}$  and  $P = 20 \text{ MPa}$ . The inset of the figure is the comparison of self-diffusion coefficients between the MD simulation results and the value calculated by using the empirical equation proposed by Vaghizadeh and Rice [32].

strongly depends on the cut-off distance. It should be noted that the curves in this figure show three distinguished features. When  $r_c = 2^{1/6}\sigma$  or the attractive forces are ignored, the RDF  $g(r)$  displays gas-like characteristic. When  $r_c \geq 1.9\sigma$ , all of the curves show the same pattern as that observed in the X-ray experimental measurement of the liquid argon [33,34]. The RDF at  $r_c = 1.5\sigma$  shows a slightly different pattern, i.e. the shape of the first valley is different from others. If the value of the first peak of the  $g(r)$  is taken as a characteristic to measure the effect of the cut-off distance on the equilibrium structure, as shown in the inset of the figure, one can see that the RDF  $g(r)$  increases quickly when  $r_c \leq 2.5\sigma$ . After that, it increases slightly and tends to plateau as the cut-off distance increases. Moreover, Figure 6 elucidates two noteworthy things. First, the WCA theory is not suitable for NPT ensembles because the second assumption of the theory, i.e. the attractive force has little influence on the RDF, is not valid in NPT ensembles. Second, it is difficult to take into account the full potential by using the cut-off potential and long-range correction because the RDF obtained by using the cut-off potential in the NPT ensemble differs from the real RDF if the cut-off distance used is not large enough.

It is well known that intermolecular forces play a key role in determining the RDF of liquid  $g(r)$  (i.e. the local packing of the liquid molecules). This is because molecules in a liquid phase are packed densely. In a gas phase, molecules are packed loosely and have a large mean free path. Intermolecular forces, especially the attractive forces between them, are weak. In this case,  $g(r)$  of a gas is dominated by molecular thermal motions. The short-range

repulsive forces between molecules have little effect on the  $g(r)$ . In the liquid phase,  $g(r)$  depends not only on molecular thermal motions and the short-range repulsive forces, but also on the long-range attractive forces. In an NPT ensemble, the volume of the system is allowed to vary; obviously, it will depend on the cut-off distance used. It is worth noting that the cut-off distance determines the extent to which the long-range attractive forces are included in the calculation. The variable volume in an NPT ensemble and the proportions of the attractive forces accounted by the cut-off distance used are the two mean reasons that cause the variation of  $g(r)$  in Figure 6.

Figure 7 shows the mean square displacements with respect to the integrating time. One can see that a shorter cut-off distance corresponds on a larger mean square displacement. The variation of the mean square displacement decreases as the cut-off distance increases. The self-diffusion coefficient calculated from the data shown in this figure was plotted in the inset of Figure 7. In this inset, the solid line with symbols  $\blacktriangle$  is the MD simulation result; the dashed line is the value calculated by using the empirical equation [32]. One can see that the difference between the results calculated using MD simulations and the empirical equation decreases as the cut-off distance increases. If the value calculated using the empirical equation is taken as the 'real value', the simulation errors at different cut-off distances are 630% at  $r_c = 2^{1/6}\sigma$ , 40% at  $r_c = 2.5\sigma$  and  $< 10\%$  for  $r_c > 4\sigma$ , respectively.

In summary, the cut-off distance used in MD simulations plays an important role in determining liquid thermodynamic properties. If the cut-off distance is chosen properly in the MD simulations, the results



obtained in the two different ensembles (NVT and NPT) will be the same and consistent with the corresponding experimental values or those calculated by using empirical equations. Ignoring the effect of the attractive forces will result in some incorrect computed results, e.g. the pressure calculated in NVT ensembles and density in NPT ensembles. For NVT ensembles with high density, the cut-off distance used in MD simulations plays little role in determining liquid structures because the liquid molecules are packed densely in a fixed volume so that there is no enough free space to allow molecules move freely. However, the volume in NPT ensembles is a free variable and the RDF in NPT ensembles varies with the cut-off distance used. The characteristic of the liquid structure being the function of the cut-off distance used in NPT ensembles indicates that the WCA theory is not suitable for NPT ensembles because of the breakdown of the assumptions applied in the WCA theory.

The WCA potential has been used to study fluid properties by many researchers [9–13]. From this study, one can see that fluid properties depend on the cut-off distance used. Ignoring the attractive forces (or using the WCA potential) leads to significant errors or incorrect results. In heterogeneous systems, it is difficult to take into account the full potential by applying the long-range correction. In this case, the Lennard-Jones potential with a larger cut-off distance should be used in order to obtain the correct results.

## 5. Conclusion

The effect of cut-off distance used in MD simulations on fluid properties was studied systematically in both NVT and NPT ensembles. Results show that the cut-off distance plays a key role in determining liquid properties, especially in NPT ensembles. To ensure that MD simulations can predict the correct results, a larger cut-off distance should be used. The characteristic of the RDF in NPT ensembles depending on the cut-off distance used means that the WCA theory is not suitable for NPT ensembles because the assumption (the effect of the attractive force in determining the liquid structure is negligible) used in the WCA theory is not valid. The dependence of fluid properties on the cut-off distance indicates that by using the WCA potential to calculate fluid transport in heterogeneous systems could lead to significant errors or incorrect results.

## Acknowledgements

The financial support from the NSERC for the authors (P.C., K.N. and L.W.K) is gratefully acknowledged. C.H. thanks the financial support from the PhD scholarship at the University of Alberta and the NSERC Postgraduate Scholarship.

## References

- [1] D. Chandler, J.D. Weeks, and H.C. Andersen, *Van der waals picture of liquids, solids, and phase transformations*, Science 220 (1983), pp. 787–794.
- [2] D. Chandler and J.D. Weeks, *Equilibrium structure of simple liquids*, Phys. Rev. Lett. 25 (1970), pp. 149–152.
- [3] J.D. Weeks and D. Chandler, *Role of repulsive forces in determining the equilibrium Structure of Simple Liquids*, J. Chem. Phys. 54 (1971), pp. 5237–5247.
- [4] L. Verlet and J.J. Weis, *Equilibrium theory of simple liquids*, Phys. Rev. A 5 (1972), pp. 939–952.
- [5] D. Beb-Amotz and G. Stell, *Reformulation of Weeks–Chandler–Andersen perturbation theory directly in terms of a hard-sphere reference system*, J. Phys. Chem. B 108 (2004), pp. 6877–6882.
- [6] M. Bishop, A. Masters, and J.H.R. Clarke, *Equation of state of hard and Weeks–Chandler–Anderson hyperspheres in four and five dimensions*, J. Chem. Phys. 110 (1999), p. 11449.
- [7] S. Hess and M. Kroger, *Pressure of fluids and solids composed of particles interacting with a short-range repulsive potential*, Phys. Rev. E 61 (2000), pp. 4629–4639.
- [8] L. Verlet, *Computer “Experiments” on classical fluids. II. Equilibrium correlation functions*, Phys. Rev. 165 (1968), pp. 201–214.
- [9] K.P. Travis and K. Gubbins, *Poiseuille flow of Lennard-Jones fluids in narrow slit pores*, J. Chem. Phys. 112 (2000), pp. 1984–1994.
- [10] X.J. Fan, N. Phan-Thien, N.T. Yong, and X. Diao, *Molecular dynamics simulation of a liquid in a complex nano channel flow*, Phys. Fluids 14 (2002), pp. 1146–1153.
- [11] L. Li, D. Bedrov, and G.D. Smith, *Repulsive solvent-induced interaction between C<sub>60</sub> fullerenes in water*, Phys. Rev. E 71 (2005), 011502.
- [12] S.R. Challa and F.V. Swol, *Molecular simulations of lubrication and solvation forces*, Phys. Rev. E 73 (2006), 016306.
- [13] A.J. Markvoort, P.A. Hilbers, and S.V. Nedea, *Molecular dynamics study of the influence of wall-gas interactions on heat flow in nanochannels*, Phys. Rev. E 71 (2005), 066702.
- [14] S.C. Jain and V.S. Nanda, *Equation of state and other associated properties of liquid argon and liquid methane*, J. Phys. C: Solid State Phys. 4 (1971), pp. 3045–3056.
- [15] C. Huang, K. Nandakumar, P. Choi, and L.W. Kostiuk, *Molecular dynamics simulation of a pressure-driven liquid transport process in a cylindrical nanopore using two self-adjusting plates*, J. Chem. Phys. 124 (2006), 234701.
- [16] C. Huang, P. Choi, K. Nandakumar, and L.W. Kostiuk, *Comparative study between continuum and atomistic approaches of liquid flow through a finite length-cylindrical nanopore*, J. Chem. Phys. 126 (2007), 224702.
- [17] C. Huang, P. Choi, K. Nandakumar, and L.W. Kostiuk, *Investigation of entrance and exit effects on liquid transport through a cylindrical nanopore*, Phys. Chem. Chem. Phys. 10 (2008), pp. 186–192.
- [18] C. Huang, P. Choi, K. Nandakumar, and L.W. Kostiuk, *Study solid wall-liquid interaction on pressure-driven liquid transport through a nanopore in a membrane*, J. Nanosci. Nanotechnol. 9 (2009), pp. 793–798.
- [19] W.G. Hoover, D.J. Evans, R.B. Hickman, A.J.C. Ladd, W.T. Ashurst, and B. Moran, *Lennard-Jones triple-point bulk and shear viscosities. Green-Kubo theory, Harniltonian mechanics, and nonequilibrium molecular dynamics*, Phys. Rev. A 22 (1980), pp. 1690–1697.
- [20] H.J.C. Berendsen, J.P.M. Postma, W.F. van Gunsteren, A. DiNola, and J.R. Haak, *Molecular dynamics with coupling to an external bath*, J. Chem. Phys. 81 (1984), pp. 3684–3690.
- [21] K. Rateitschak, R. Klages, and W.G. Hoover, *The Nose-Hoover thermostated Lorentz gas*, J. Stat. Phys. 101 (2000), pp. 61–77.
- [22] G. Drazer, J. Koplik, and A. Acrivos, *Adsorption phenomena in the transport of a colloidal particle through a nanochannel containing a partially wetting fluid*, Phys. Rev. Lett. 89 (2002), 244501.
- [23] J. Koplik, J.R. Banavar, and J.F. Willemsen, *Molecular dynamics of fluid flow at solid surfaces*, Phys. Fluids A1 5 (1989), pp. 781–794.
- [24] I. Bitsanis, J.J. Magda, M. Tirrell, and H.T. Davis, *Molecular dynamics of flow in micropores*, J. Chem. Phys. 87 (1987), pp. 1733–1750.

- [25] P.A. Thompson and S. Troian, *A general boundary condition for liquid flow at solid surfaces*, Nature 389 (1997), p. 360.
- [26] M. Cieplak, J. Koplik, and J.R. Bavanar, *Boundary conditions at a fluid–solid interface*, Phys. Rev. Lett. 86 (2001), pp. 803–806.
- [27] L. Xu, M.G. Sedugh, M. Sahimi, and T.T. Tsotsis, *Nonequilibrium molecular dynamics simulation of transport of gas mixtures in nanopores*, Phys. Rev. Lett. 80 (1998), pp. 3511–3514.
- [28] R.F. Cracknell, D. Nicholson, and N. Quirke, *Direct molecular dynamics simulation of flow down a chemical potential gradient in a slit-shaped micropore*, Phys. Rev. Lett. 74 (1995), pp. 2463–2466.
- [29] J. Weng, S. Park, J.R. Lukes, and C. Tien, *Molecular dynamics investigation of thickness effect on liquid films*, J. Chem. Phys. 113 (2000), pp. 5917–5923.
- [30] J.H. Irving and J.G. Kirkwood, *The statistical mechanical theory of transport processes. IV. The equations of hydrodynamics*, J. Chem. Phys. 18 (1950), pp. 817–829.
- [31] W. Yu, Z.Q. Wang, and D. Stroud, *Empirical molecular-dynamics study of diffusion in liquid semiconductors*, Phys. Rev. B 54 (1996), pp. 13946–13954.
- [32] J. Naghizadeh and S.A. Rice, *Kinetic theory of dense fluids. X. Measurement and interpretation of self-diffusion*, J. Chem. Phys. 36 (1962), pp. 2710–2720.
- [33] A. Eisenstein and N.S. Gingrich, *The diffraction of X-rays by argon in the liquid, vapor, and critical regions*, Phys. Rev. 62 (1942), pp. 261–270.
- [34] B.J. Yoon, M.S. Jhon, and H. Eyring, *Radial distribution function of liquid argon according to significant structure theory*, Proc. Natl Acad. Sci. USA 78 (1981), pp. 6588–6591.